PNAS

Supporting Information for

PHGDH preserves one-carbon cycle to confer metabolic plasticity in chemo-resistant gastric cancer during nutrient stress

Bo Kyung Yoon[1,2,3,*], Hyeonhui Kim[1,*], Tae Gyu Oh[4], Se Kyu Oh[5], Sugyeong Jo[1], Minki Kim[1], Kyu-Hye Chun[1,2,3], Nahee Hwang[1,2,3], Suji Lee[1], Suyon Jin[1], Annette R. Atkins[4], Ruth T. Yu[4], Michael Downes[4], Jae-woo Kim[1,2,3,†], Hyunkyung Kim[6,7,†], Ronald M Evans[4,†], Jae-Ho Cheong[1,2,3,8,9,10,†] and Sungsoon Fang[1,5,11,†]

† Correspondence:
Jae-woo Kim: japol13@yuhs.ac
Hyunkyung Kim: hyunkkim@korea.ac.kr
Ronald M Evans: evans@salk.edu
Jae-Ho Cheong: jhcheong@yuhs.ac
Sungsoon Fang: sfang@yuhs.ac

This PDF file includes:

Supplementary Information Text

Materials and Methods

Cell culture. MKN1, SNU601, and NCIN87 cells were cultured in RPMI1640 containing 10 % fetal bovine serum (FBS), 2 mM L-glutamine, 100 U/ml penicillin, and 100 μg/ml streptomycin. HS746T cells were cultured in DMEM containing 10 % FBS, 2 mM L-glutamine, 100 U/ml penicillin and 100 μg/ml streptomycin. Cells were cultured in a humidified 5 % CO2 atmosphere at 37 °C. All cell lines were tested for mycoplasma contamination.

Organoid culture. Organoids were generated and maintained as previously described with minor modifications(1). Gastric fundus organoids were derived from surgical samples from GC patients with informed consent received at the Yonsei University Severance Hospital (IRB No. 4-2017-0106). The sampled tissue was then mixed in matrigel (BD Biosciences) and plated in 48-well plates. Culture conditions are as follows: Advanced Dulbecco's modified Eagle medium/F12 medium (Invitrogen), R-spondin-conditioned medium, and Wnt-conditioned medium supplemented with gastric growth factors including bone morphogenetic protein inhibitor, noggin (PeproTech), GlutaMAX-I (Invitrogen), B27 (Invitrogen), TGF beta I A83-01 (TOCRIS), Nicotinamide (Sigma), N-acetylcysteine (Sigma), gastrin (Sigma), epidermal growth factor (PeproTech), and fibroblast growth factor 10 (R&D systems). The cells matured into organoids after 1–2 days. Gastric organoids were subsequently passaged every 6 to 8 days depending on the size of organoids. Organoid size was measured as an average of shortest and longest diameters crossing the center of organoids.

ATAC sequencing analysis. HS746T and NCIN87 cells deprived of glutamine for 48 hr were prepared as a single cell suspension using trypsin-EDTA. Cells were counted using LUNA-FL™ Automated Fluorescence Cell Counter (Logos Biosystems). After cell lysis, the nuclei concentration was measured with Countess II Automated Cell Counter (ThermoFisher) and nuclei morphology was examined. After lysis, we continued to the transposition reaction. Nuclei (50,000 cells) were re-suspended in transposition reaction mix and incubated for 30 min at 37 °C. Immediately following the transposition process, the sample was purified using a Qiagen MinElute PCR purification Kit. Transposed DNA fragments was amplified using Nextera DNA Flex kit. A qPCR side reaction was run with appropriate number of cycles to reduce GC and size bias. The amplified library was purified, quantified with Quantification Protocol Guide (KAPA), and quality confirmed with Bioanalyzer (Agilent technologies). Libraries were sequenced using the HiSeq platform (Illumina). The experiment was run in duplicates. Peaks were called with the aligned sequence data using a model-based analysis of ATAC-seq (MACS2 version 2.1.1) (2). Parameters used are as follows; macs2 callpeak -t ATAC-seq.bam -g hs --bdg --nolambda --keep-dup all --broad. Among the called peaks, the peaks overlapping with ENCODE blacklisted regions were removed. ChIPseeker package (version 1.20.0) (3) was used to identify nearby genes and transcripts from the peaks obtained from MACS2. Heatmap of the normalized signal intensity across genomic regions was drawn with deepTools (4).

Single-nucleus RNA sequencing analysis. After the frozen tissue was homogenized and nuclei were counted, the nuclei were isolated using Flow Cytometry. We utilized the 10X Genomics Chromium Instrument and cDNA synthesis kit (10x Genomics: Chromium Next GEM Automated Single Cell 3′ Library and Gel Bead Kit v3.1) to generate a barcoded cDNA library for single Nuclei RNA-sequencing from approximately 4882 nuclei. cDNA library quality was determined using an Agilent Bioanalyzer. Using this library, we ran two paired-end 100bp Flow Cells on an Illumina Novaseq 6000. Demultiplexed fastq files were generated and aligned to the mouse genome using the 10X Genomics Cellranger with the option --force-cells 2000. Cellranger outcomes were loaded to the R package using read10X function of Seurat (5) and the pipeline from the package was utilized to detect gene expression and clusters. To perform

quality control and select cells for further analysis, cells were filtered with the cutoff as follows; number of Feature per cell is between 200 and 5000, number of UMI per cell is below 20,000 and percent of mitochondria is lower than 10%. For normalization and scale, the default setting was used. In order to remove batch effect among samples, we used FindIntegrationAnchors and IntegrateData commands as canonical correlation analysis (CCA) of the Seurat. Clustering was performed using FindClusters function of the Seurat with the options of 0.6 resolution and integrated DefaultAssay. To achieve dimensional reduction, RunUMAP function was utilized. Each cluster was defined with the previous marker genes. To visualize the marker genes, FeaturePlot or DimPlot functions were utilized. For further analysis of cell population with restored expression, we utilized the expression recovery algorithm, ALRA (6). The RunALRA command of the Seurat Wrapper package was used with the default setting. To examine the expression pattern of genes, we used FindMarkers or FindAllMarkers function from the Seurat using the default setting. Furthermore, average expression was calculated with the AverageExpression command. Cell counting was performed using sample and cell information from the Seurat meta.data. To examine stemness potency, the entropy score was computed using the SCENT package (7). Briefly, the ALRA counts were extracted. Then, transcript annotation was matched using the org.Hs.eg.db library. The DoIntegPPI and CompSRana commands were applied to generate entropy scores. To examine the single cell trajectory, the Slingshot package was utilized. The pseudotime/trajectory was computed with the slingshot and slingPseudotime command with setting the cluster 8 as a start.clust. All SCENT and slingshot outcome were established and matched with the original 10X outcome including clusters and UMAP dimensions. To visualize the trajectory of RNA samples, the plot function with slingshot reduceDim scores was utilized. To compute regulatory network and regulon activity, SCENIC package was used (8). Cell-cell communication was computed using CellChat package (9).

Chromatin immunoprecipitation assay. Chromatin and proteins were cross-linked with 1% (w/v) methanol-free formaldehyde (28908, Thermo) at room temperature for 5min and then added 0.125M final concentration of glycine to stop cross-linking. The cells were washed with cold PBS and harvested by cell lysis buffer (150mM NaCl, pH7.8 50mM Tris-HCl, pH7.6 5mM EDTA, 0.5% NP-40, 1% Triton X-100, 1X protease inhibitor). The cell suspension was aspirated and pushed through a 1ml insulin syringe to break apart cell membranes and centrifuged at 12000g for 1min at 4 °C. The pellet was resuspended to shearing buffer (1% SDS, pH 7.6 10mM EDTA, pH 8.0 50mM Tris-HCl, 1X protease inhibitor) and chromatin shearing was performed through Covaris ultrasonicator (M220). Diluted samples to Dilution buffer (150mM NaCl, pH 8.0 20mM Tris-HCl, pH 7.6 2mM EDTA, 1% Triton X-100, 1X protease inhibitor) were immunoprecipitated using control antibody rabbit IgG (2729, Cell signaling technology), ATF4 (11815, Cell signaling technology), CEBPB (sc-7962, Santa Cruz biotechnology), acetyl histone H3 (06-599, Millipore) and incubated with protein A and protein G bead slurry for 1hr at 4°C. The antibody-chromatin complexes were washed buffer 1 (150 mM NaCl, pH 8.0 20 mM Tris-HCl, pH 7.6 2 mM EDTA, 0.1 % SDS, 1 % Triton X-100), buffer 2 (500 mM NaCl, pH 8.0 20 mM Tris-HCl, pH 7.6 2 mM EDTA, 0.1 SDS, 1 % Triton X-100), buffer 3 (0.25 M LiCl, pH 8.0 10 mM Tris-HCl, pH 7.6 1 mM EDTA, 1 % NP-40, 1 % deoxycholate), and TE buffer (pH 8.0 10 mM Tris-HCl, pH 7.6 1 mM EDTA) 3 times continuously. The crosslinking was reversed by incubation with elution buffer (1% SDS, pH 8.0 50mM Tris-HCl, pH 7.6 50 mM EDTA) at 65°C overnight followed by incubation with proteinase K. DNA was purified with a QiAquick PCR purification Kit (QIAGEN 28106). Purified DNA was analyzed by quantitative PCR with following primers; PHGDH +741 F: CGTAAGGCAGCAAACACGTA, R: GTGGGGAGGAGGCTAAATCT; SHMT2 +463 F: CGGGTAGGGGGCTAAGTAAG, R: GTGGGAGGGGAGACCTTTAG; MTHFD2 +676 F: ACTCTGGGCACCCTAGCTTT, R: CGGATGTTTGCCACCTCTAT; ASNS -87 F: TGGTTGGTCCTCGCAGGCAT, R: CGCTTATACCGACCTGGCTCCT; ASNS exon F: GCAGCTGAAAGAAGCCCAAGT, R : TGTCTTCCATGCCAATTGCA.

Chromatin immunoprecipitation sequencing analysis. For ATF4 and CEBPB ChIP-seq of HS746T cells, 10^7 cells were collected for each condition. Samples were prepared similar to the ChIP assay. ChIP'd DNA was quantified using Quant-IT PicoGreen (Invitrogen) and qualified using the Agilent High Sensitivity DNA Kit on Agilent 2100 Bioanalyzer (Agilent Technologies). The libraries were prepared according to the manufacturer's instructions of the TruSeq ChIP Sample Preparation Kit (Illumina). In brief, 10 ng of ChIP'd DNA is end-repaired to create dsDNA molecules (5'-phosphorylated and blunt-ended). Following the end-repair, these DNA fragments undergo the addition of a single 'A' base and ligation of the TruSeq indexing adapters. Next, the products are purified and enriched with PCR and final DNA library is created. The libraries were quantified according to the qPCR Quantification Protocol Guide (KAPA Library Quantification kits for Illumina Sequencing platforms) and qualified using the TapeStation D1000 ScreenTape (Agilent Technologies). Indexed libraries were sequenced with the HiSeqX™ platform (Illumina) by the Macrogen Incorporated.

NADP and NADPH quantification. Intracellular NADP and NADPH concentrations were determined using NADP/NADPH Quantitation Kit (MAK038, sigma) according to the manufacturer's instructions. Briefly, counted cell pellet was dissolved with NADP/NADPH extraction buffer and centrifuged at 10000g for 10 min at 4 °C. The supernatant was filtered with Amicon Ultra-2 Centrifugal Filter Unit (UFC201024, Millipore) through centrifuging at 5400g for 15min at 4 °C. The filtered samples were used for total NADP and heated samples (60 °C for 30 min) were used for NADPH quantification. Color changes were measured with a Thermo spectrophotometric multiwell plate reader. According to the NADPH standards, the concentration of total NADP or NADPH can be expressed in picomole per 10^6 cells.

GSH and GSSG quantification. HS746T cells were plated into 96-well plates, and deprived of glutamine or treated NCT-503 25 μM for 48 hr. GSH/GSSG ratio was quantified using GSH/GSSG-Glo™ Assay (V6611, Promega) according to the manufacturer's instructions. Briefly, culture media was removed and cells were dissolved at total glutathione lysis reagent or oxidized glutathione lysis reagent. After incubation for 5min, luciferin generation reagent and luciferin detection reagent were added and measured luminescence with Centro XS3 LB960 (EG & G Berthold). Using the standard curve, luminescence was converted to micromoles of GSSG and GSH. The GSH/GSSG ratio was calculated using the following formula: GSH/GSSG ratio = (total glutathione – GSSG*2)/GSSG.

Mitochondria extraction. Cytosolic, mitochondrial fractions were prepared using Mitochondria Isolation Kit for Cultured Cells (89874, Thermo) according to the manufacturer's instructions. Briefly, the harvested cell suspension was centrifuged at 850g for 2 min at 4 °C and lysed in mitochondria isolation reagent. cell lysis centrifuged at 850g for 5 min at 4 °C. The pellet was discarded, and the supernatant was centrifuged at 12000g for 15min at 4 °C. The supernatant was stored, and the pellet was washed with reagent C. For analysis by western blotting, the mitochondrial pellet was lysed with RIPA buffer, and the protein concentration of each fraction were measured using a BCA protein assay kit (23225, Thermo).

Measurement of intracellular ROS and mitochondrial ROS level. The intracellular ROS level was determined using DCFDA (Invitrogen) and mitochondrial ROS level was determined using MItoSOX (invitrogen). HS746T cells were into plated into 96-well or 12-well plates and deprived of glutamine or treated NCT-503 25 μM for 48 hr. after incubation, cells were washed with 10 % FBS DMEM without phenol red and incubated with 20 μM DCFDA for 30 min at 37 °C or 5 μM MitoSOX for 5 min at 37 °C. At the end of the incubation, media suction and cell washed with 10 % FBS DMEM without phenol red. 96-well plate fluorescence intensity measured by Varioskan Flash 3001 fluorometer (Thermo). The fluorescence value was calculated after excluding the value of no cell control. 12-well plated fluorescence intensity captured by Fluorescent inverted microscope (Olympus, IX73).

shRNA stable cell line generation. TRCN0000028548 shRNA construct targeting PHGDH was purchased from the Yonsei system biology core TRC shRNA service. To generate lentiviruses, HEK-293T were transfected with pMD2.G, psPAX2, and pLKO.1 shRNA vector using FuGENE HD transfection reagent (promega, E2311) following the manufacturer's protocol. After 24hr, the media was replaced with the fresh culture media and the media containing lentiviral particles was collected. HS746T cells were infected with viral supernatant and selected with 1 μg/ml puromycin.

siRNA knockdown. SiRNAs were purchased from Santa Cruz Biotechnology (ATF4: sc-35112, CEBPB: sc-29229, control A: sc-37007). 50nM siRNAs were transfected into HS746T cells using Lipofectamine RNAiMAX (Invitrogen) following the manufacturer's protocol.

Immunoblotting. For the western blot assay, cells were scraped and lysed in EBC200 buffer (0.2M NaCl, 0.05M Tris-HCl pH 8.0, 0.5% NP-40, 1X protease inhibitor cocktail, 1X phosphatase inhibitor cocktail). The protein concentration was determined by the BCA assay kit (Pierce, 23225). Total protein (20ug) was separated by SDS-PAGE and then transferred to PVDF membranes. Primary antibodies used were GLS(Proteintech, 12855-1-AP), PHGHD(Santa Cruz Biotechnology, sc-100317) SHMT1(Santa Cruz Biotechnology, sc-365203), SHMT2(Santa Cruz Biotechnology, sc-390641), MTHFD2, H3(abcam, ab1791), beta-actin(Santa Cruz Biotechnology, sc-47778), COX4(Cell Signaling Technology, 4850s), alpha-tubulin(Santa Cruz Biotechnology, sc-8035), ATF4(Cell Signaling Technology, 11815), CEBPB (Santa Cruz Biotechnology, sc-7962), CHOP(Proteintech, 15204-1-AP), p-eIF2a(Cell Signaling Technology, 9721), eIF2a(Cell Signaling Technology, 9722), p-IRE1(Abcam, ab48187), IRE1(Abcam, ab37073).

Quantification of mRNA expression level. For mRNA expression quantification, total RNA was isolated from cells or organoid samples by TRIzol (Invitrogen). The amount of RNA was determined using a NanoDrop (Thermo and cDNA was synthesized from 2ug RNA with GoScript™ Reverse Transcriptase (Promega, A5003). Real-time PCR was performed with TOPreal™ qPCR 2X PreMIX (enzynomics, RT500) using CFX Connect Real-Time PCR System (Bio-rad) and the relative amounts of mRNAs were calculated using the comparative CT method. 36B4 gene was used as a control. Values show the amount of mRNA relative to the control sample. Primers are listed in the supplementary information.

Cell proliferation assay. 96-well plated cells were treated with chemicals or changed to starvation media. Medium was removed and plate frozen at -80 °C at every time point. After finishing sample collection, plates were thawed and DNA content was measured by CyQUANT™ Cell Proliferation Assay, for cells in culture (C7026, Invitrogen). according to the manufacturer's instructions. Briefly, cell lysis solution with dye was added to the plate and incubated for 5 min at room temperature protected from light. Fluorescence was measured by Varioskan Flash 3001 fluorometer (Thermo).

In vivo peritoneal dissemination model. The construction of mice GC peritoneal dissemination model was approved by the institutional animal care and use committee of the Yonsei University College of Medicine (2021-0324). Mice were acclimated for at least 7 days under a 12 hr light/12 hr dark cycle. Puromycin-resistant HS746T-mCherry cell line was generated from incubation in media containing lentivirus produced by cotransfecting pLL-mCherry-puro (kind gift from Kyung-Sup Kim), pMD2.G, and psPAX2 in 293T human embryonic kidney cells. HS746T-mCherry (2 × 106 cells) was injected intraperitoneally in BALB/ c-nude mice. After 7 days of cell injection, mice were divided into 4 groups (n=7, each) randomly for BPTES and NCT503 treatment. Mice were injected intraperitoneally with vehicle (20% (v/v) DMSO, 50% (v/v) PEG-400, and 30% (v/v) PBM) or 12.5 mg/kg of BPTES for one day followed by injection of vehicle or 40 mg/kg of NCT503 for two days (1st cycle). It was

repeated after one day of break (2nd cycle). 3rd cycle of drug injection was performed 7 days after the 2nd cycle. Tumor volume was recorded via in vivo optical imaging system (IVIS).

S-Adenosylmethionine (SAM) quantification. Gastric cancer cells were collected with the same cell number, and sonicated using UP200St Ultrasonic Lab Homogenizer (Hielscher) 20cycles of 40 sec at 30% amplitude under 1 sec in 500ul cold PBS. Cell lysates were centrifuged at 10,000g for 15 min at 4°C. The pellet was discarded, and the supernatant was stored for use into the assay. S-Adenosylmethionine (SAM) levels of GC cell lines were measured using the S-Adenosylmethionine (SAM) and S-Adenosylhomocysteine (SAH) ELISA Combo Kit (STA-671-C, Cell Biolabs) following the manufacturer's protocol. Intracellular SAM concentration (ug/mL) determined using a standard curve and normalized to protein concentration using the BCA assay.

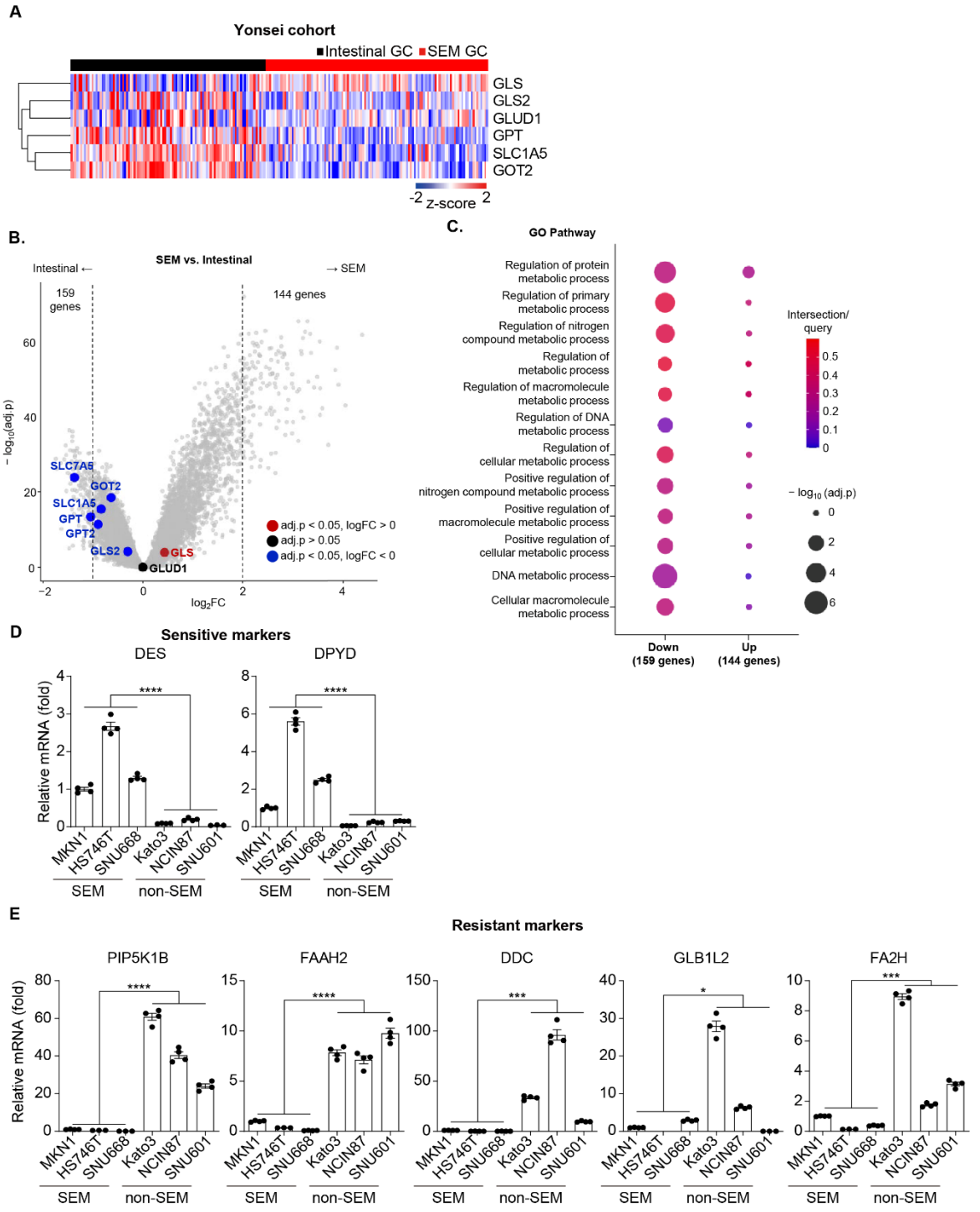

Fig. S1. SEM-type GC cells are predicted to be sensitive to GLS inhibition. (A) Transcriptome profile of tumors of GC patients in the Yonsei cohort. The expression level of glutaminolysis-related genes is compared according to the subtype: SEM (n = 117) and intestinal (n = 102). (B) Transcriptomic profiles of GC patients in the Yonsei cohort. There are 144 genes with a fold change greater than 2 with an adjusted p-value less than 0.05 and 159 genes with a fold change less than -1 with an adjusted p-value less than 0.05. (C) GO Pathway analysis on up-regulated 144 genes (log2FC > 2) and down-regulated 159 genes (log2FC < −1) (D, E) mRNA expression level of resistant markers (PIP5K1B, FAAH2, DDC, GLB1L2, and FA2H) and sensitive markers (DSE and DPYD) for GLS inhibition. *p < 0.05, ***p < 0.001, ****p < 0.0001

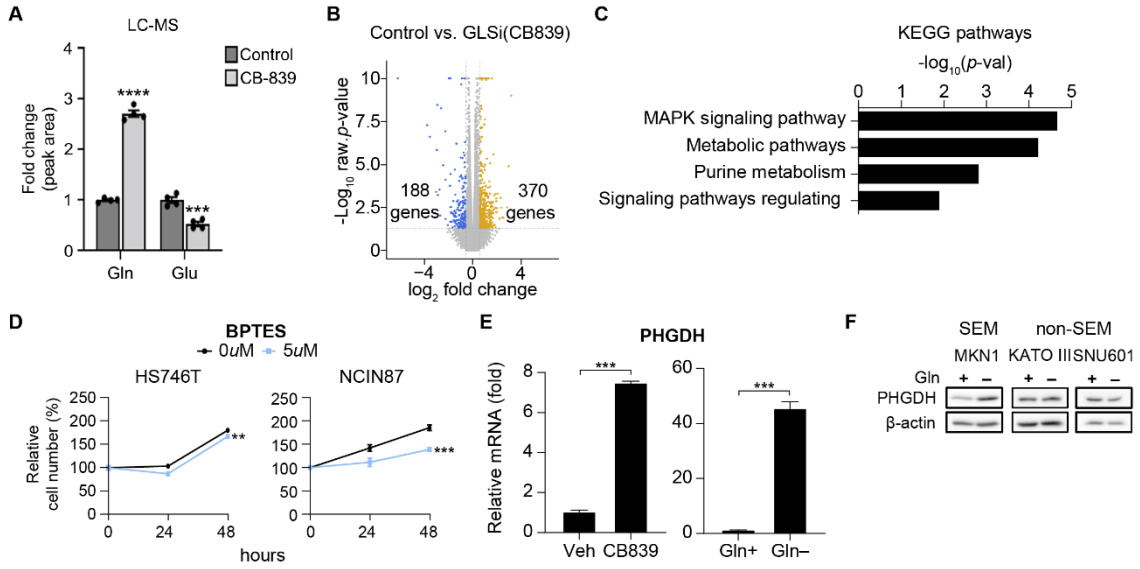

Fig. S2. Pharmaceutical inhibition of GLS up-regulated PHGDH. **(**A) The amount of intracellular glutamate and glutamine were measured by liquid chromatography-mass spectrometry analysis technique. (B) Transcriptomic profile of CB839 treated HS746T was analyzed using mRNA sequencing analysis. Genes with fold change greater than 1.5 and raw p-values smaller than 0.05 are marked in yellow. Genes with fold change less than -1.5 and raw p-values smaller than 0.05 are marked in blue. (C) KEGG analysis with differentially expressed genes (DEGs) with p-values less than 0.05. Each pathway includes more than five DEGs. (D) Proliferation assays were performed for 48 hr in HS746T and NCIN87 cells under glutamine-deficient and drug-treated conditions. BPTES; GLS inhibitor. (E) mRNA expression level of PHGDH with or without CB839 treatment in HS746T cells. (F) Immunoblot showing the protein levels of PHGDH upon glutamine starved MKN1, KATO III, SNU601 cells. β-actin was used as a loading control. ns, no significant difference, **p < 0.01, ***p < 0.001, ****p < 0.0001

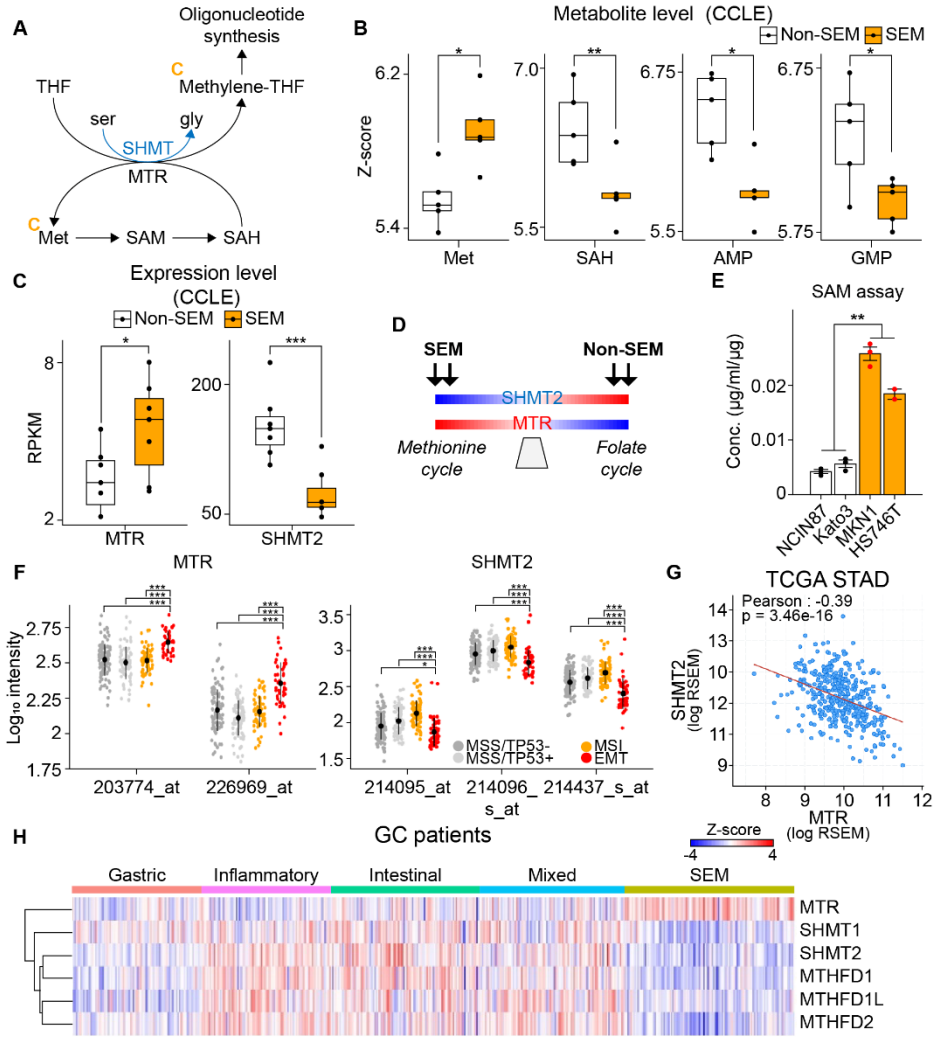

Fig. S3. SEM-type GC shows distinct 1C metabolism compared to non-SEM GC. (A) Schematic of folate cycle and methionine cycle coupled to run 1C metabolism. (B) Analyses of Cancer Cell Line Encyclopedia(CCLE) metabolomics dataset to show the intracellular amounts of methionine, 5-adenosylhomocysteine(SAH), AMP, and GMP. SEM-type GC cell lines with metabolomics data listed include HS746T, MKN1, MKN74, SNU1, and SNU668. non-SEM type GC cell lines include KATOIII, SNU601, NCIN87, SNU16, and SNU620. (C) RNAseq gene expression data from CCLE. Expression levels are indicated by RPKM values. SEM-type GC cell lines include HS746T, MKN1, MKN74, SNU1, SNU638, SNU668, and SNU484. non-SEM type GC cell lines include KATOIII, SNU601, NCIN87, SNU16, SNU620, SNU719, and YCC3. (D) Schematic of SEM and non-SEM type GC with emphasis on different cycles of 1C metabolism predicted with transcriptomic and metabolomics data. (E) The amount of intracellular SAM was measured and normalized. (F) The expression levels of MTR and SHMT2 transcripts were compared in the patients with different molecular subtypes in the Asian Cancer Research Group cohort (GSE62254). (G) Pearson correlation analysis between SHMT2 and MTR in TCGA STAD. (H) A heatmap showing folate cycle-related genes and MTR. *p < 0.05, **p < 0.01, ***p < 0.001

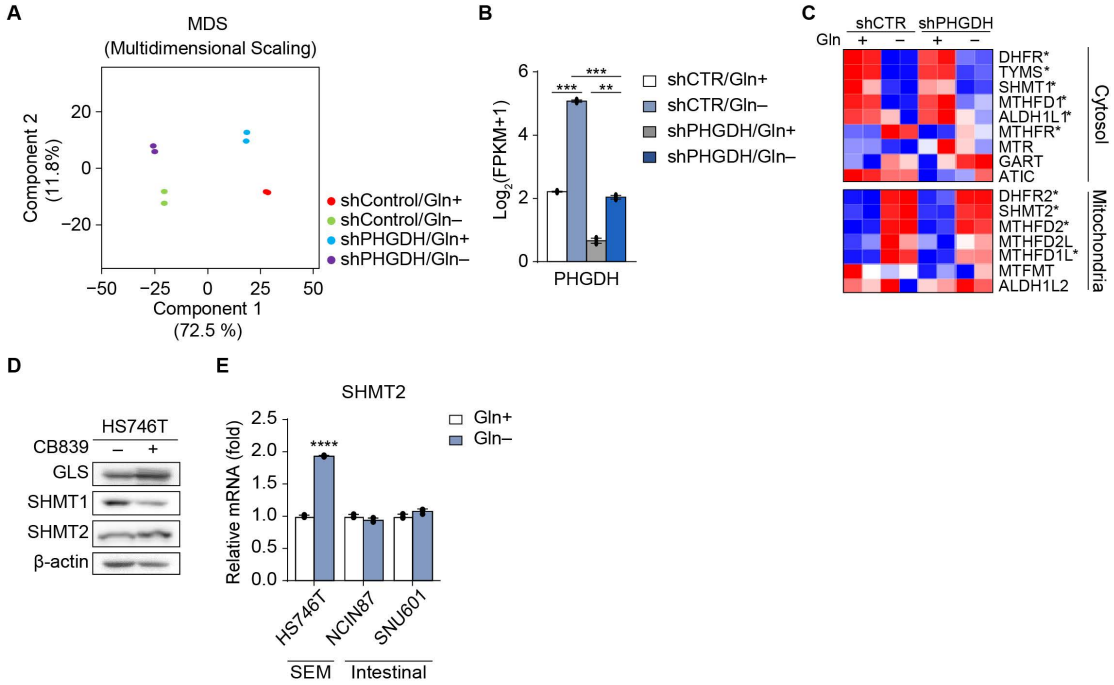

Fig. S4. Glutamine starvation up-regulates mitochondrial isoform of folate cycle-related genes. (A) RNA sequencing was performed on shControl or shPHGDH stable HS746T cell line with or without glutamine. Multidimensional scaling plot of samples based on RNA-seq data. (B) The expression level of PHGDH in log2(FPKM+1) value in shControl or shPHGDH stable HS746T cell line with or without glutamine. (C) Heatmap shows folate cycle-related genes with FPKM values. Cellular localization of each gene is marked on the right. (D) Immunoblot showing the protein levels of GLS, SHMT1, and SHMT2 upon 5 μM CB839 treated HS746T cells. β-actin was used as a loading control. (E) The relative mRNA expression level of SHMT2 in fold change. *p < 0.05, **p < 0.01, ***p < 0.001, ****p < 0.0001

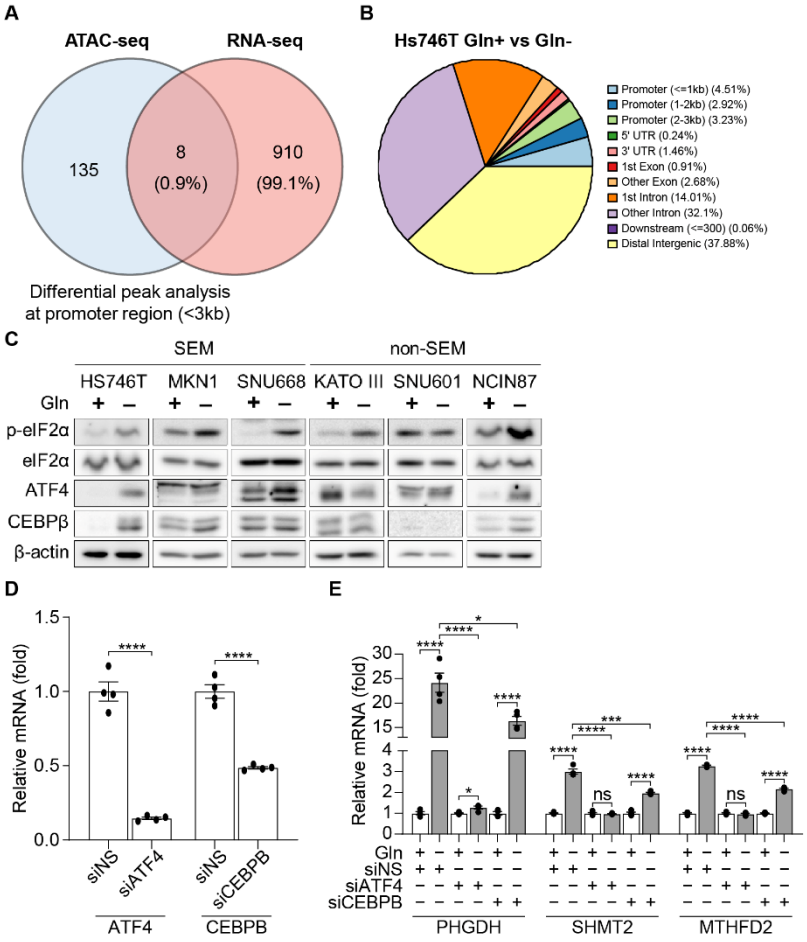

Fig. S5. ATF4 or CEBPB knockdown blocks activation of PHGDH-driven salvage pathway. (A) Venn Diagram shows the overlap between differentially accessible ATAC peaks at promoter region and differentially expressed genes at RNA seq. (B) Visualization of genomic annotation regions. (C) Immunoblot showing the protein levels of p-eIF2α, eIF2α, ATF4 and CEBPB upon glutamine-starved HS746T, MKN1, SNU668, SNU601, KATO III, NCIN87 cells. β-actin was used as a loading control. (D) mRNA expression levels of ATF4 and CEBPB were shown after knockdown with siRNA to show knockdown efficiency. (E) The relative mRNA expression levels of PHGDH, SHMT2, and MTHFD2 with ATF4 or CEBPB knockdown along with glutamine starvation. ns, no significant difference, *p < 0.05, ***p < 0.001, ****p < 0.0001

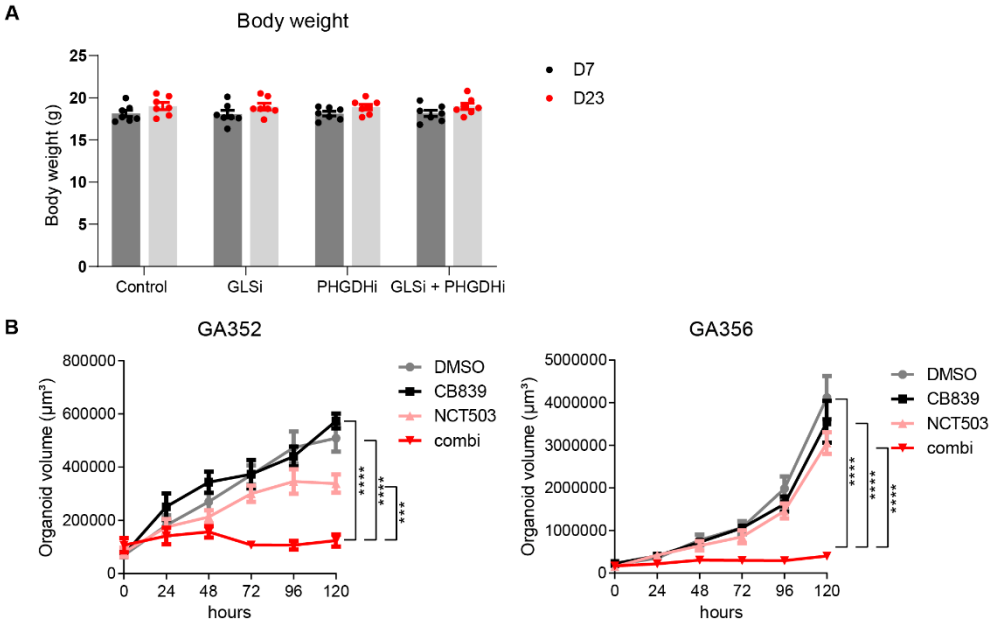

Fig. S6 Efficiency of combinational therapy in *in vivo* models and patient-derived cancer organoids. (A) Effect of drugs on mouse body weight. n = 7 mice/group. There was no statistically significant difference between groups. (B) Calculated volume (n = 8, each) of the SEM patient-derived cancer GA352, GA356 before and after drug treatments.

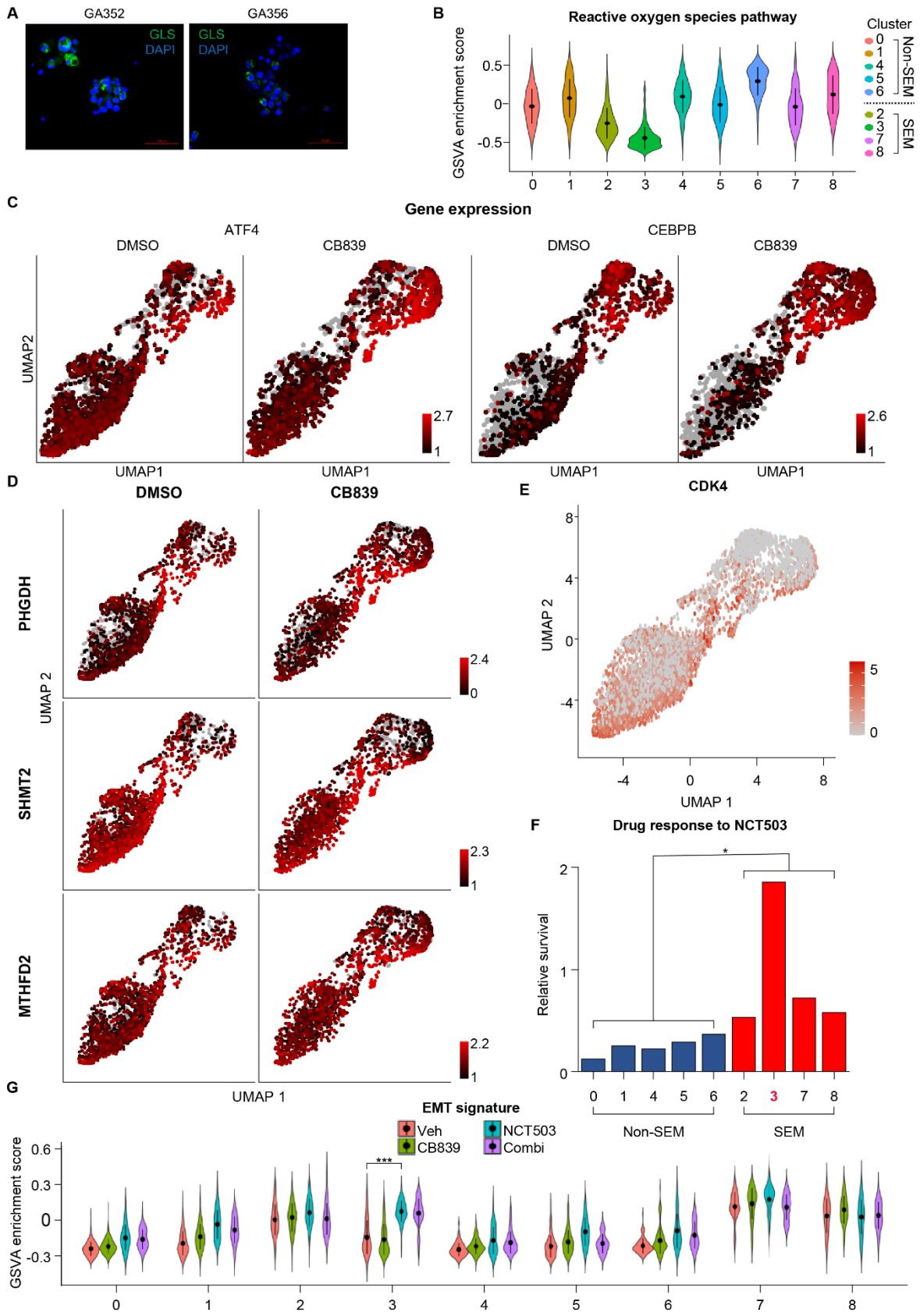

Fig. S7. Single-nucleus RNA sequencing analysis of the patient-derived organoid shows intratumoral heterogeneity contributing to different sensitivities to the drug. (A) Immunocytochemistry image of GLS in SEM patient-derived cancer organoids GA352, GA356 stained with DAPI. Scale bar: 50 μm. (B) GSVA analysis was performed to calculate enrichment score with GO pathway

“GO_REACTIVE_OXYGEN_ SPECIES_PATHWAY” from MSigDB v7.4. SEM vs non-SEM : p-val < 0.0001 (C) Expression levels of ATF4 and CEBPB were plotted on the corresponding UMAP. (D) The expression levels of PHGDH, SHMT2, and MTHFD2 were plotted on the corresponding UMAP. Cells treated with CB839 were compared with control cells. (E) The expression level of CDK4 was plotted on the corresponding UMAP. (F) Relative survival on NCT503 treatment was calculated as number of cells in each cluster divided by number of cells in the control group. (G) GSVA analysis was performed in different conditions in each cluster with EMT signature (Hallmark) from MsigDB v7.4. *p < 0.05, ***p < 0.001, Wilcox test for S7B, S7G, Two-tailed student's t test for S7F

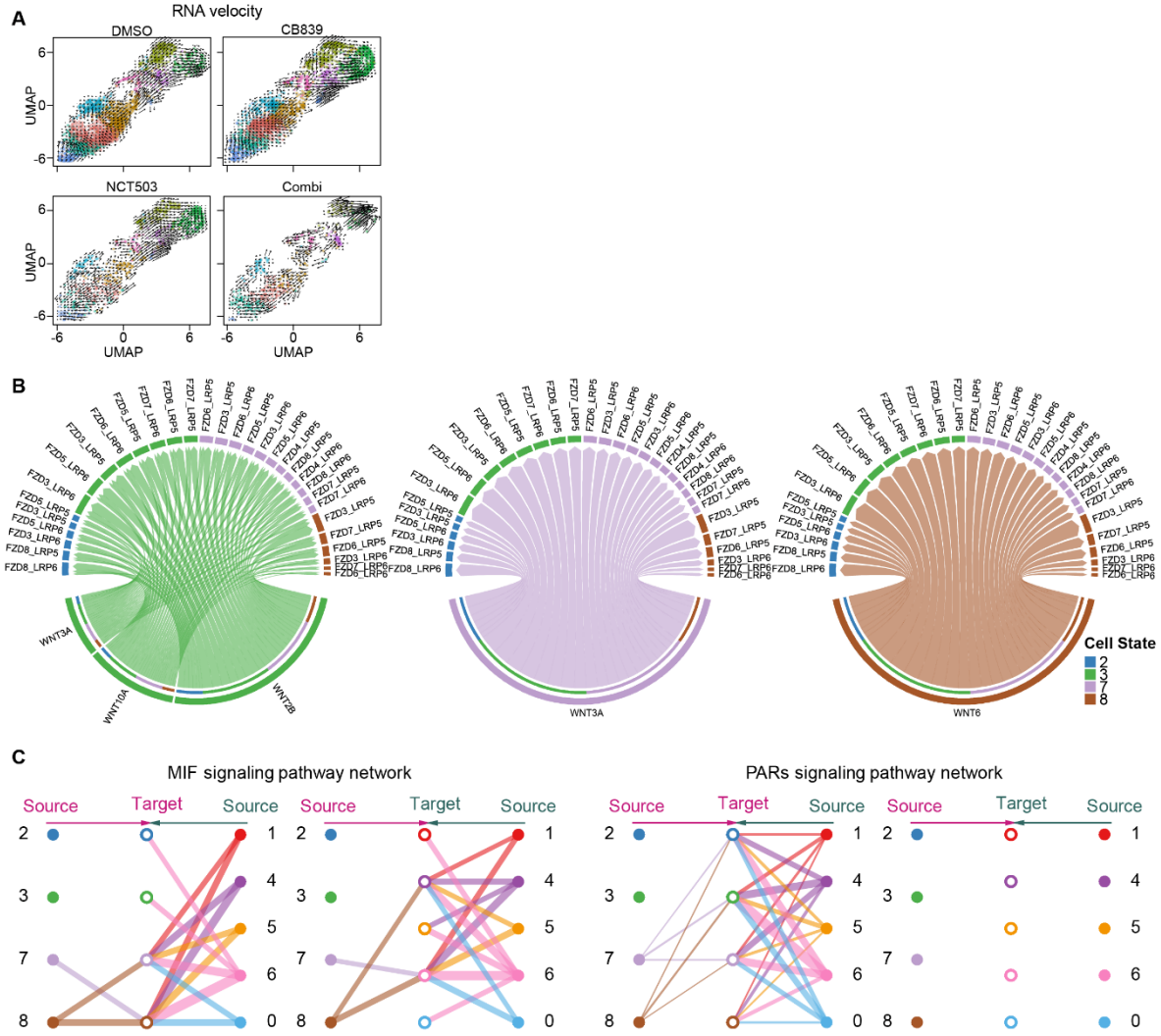

Fig. S8. Cells in the patient-derived organoids show different levels of stemness. (A) RNA velocity at the single-cell level was estimated across a population of cells and marked as an arrow on the corresponding UMAP plot. (B) Inferred ligand-receptor communication in WNT signaling pathway. Edge width means communication probability and edge color represents different clusters (2, 3, 7, and 8). (C) Hierarchical plot shows the inferred intracellular network for MIF signaling pathway and PARs signaling pathway. The color of the circles differing among clusters and edge width means the communication probability.

qPCR primers		
Gene		**Sequence (5' → 3')**
PHGDH	F	CTGCGGAAAGTGCTCATCAGT
	R	TGGCAGAGCGAACAATAAGGC
SHM1	F	AGGAAAGGAGTGAAAAGTGTGGAT
	R	GACACCAGTGTCGCTCTGGATCTG
SHMT2	F	ATGTCTATGCCCTATAAGCTCAACCC
	R	GCCGGAAAAGTCGAGCAGT
MTHFD2	F	AGGACGAATGTGTTTGGATCAG
	R	GGAATGCCAGTTCGCTTGATTA
ATF4	F	CCCTTCACCTTCTTACAACCTC
	R	TGCCCAGCTCTAAACTAAAGGA
CEBPB	F	CTTCAGCCCGTACCTGGAG
	R	GGAGAGGAAGTCGTGGTGC
DSE	F	GGGCTCCCAGTGTGTTTTTCA
	R	ATGGCTGTCGTAGTTGGCATT
DPYD	F	GGCGGACATCGAGAGTATCCT
	R	TTCTTGGCCGAAGTGGAACAC
PIP5K1B	F	TGACCCCAGCACATCACTAC
	R	GCTCCAGGGTTAGACAGTTCT
FAAH2	F	CATAGGCTTAGTAGGCCGAGC
	R	CTTTCTCTGTCGGATCAGCTTG
DDC	F	TGGGGACCACAACATGCTG
	R	TCAGGGCAGATGAATGCACTG
GLB1L2	F	CGAAGCAGTGGACCTTTATTTTG
	R	GCATGTATGCGGGGTCTTTAT
FA2H	F	GTACGATGAGTGGGTTCACCA
	R	GATGGGGACACTGTACCAGAC

Table S1. list of qPCR primers used in the study

SI References

1. S. Bartfeld *et al.*, In vitro expansion of human gastric epithelial stem cells and their responses to bacterial infection. *Gastroenterology* **148**, 126-136 e126 (2015).
2. Y. Zhang *et al.*, Model-based analysis of ChIP-Seq (MACS). *Genome Biol* **9**, R137 (2008).
3. G. Yu, L. G. Wang, Q. Y. He, ChIPseeker: an R/Bioconductor package for ChIP peak annotation, comparison and visualization. *Bioinformatics* **31**, 2382-2383 (2015).
4. F. Ramirez *et al.*, deepTools2: a next generation web server for deep-sequencing data analysis. *Nucleic Acids Res* **44**, W160-165 (2016)
5. T. Stuart *et al.*, Comprehensive Integration of Single-Cell Data. *Cell* **177**, 1888-1902 e1821 (2019).
6. G. C. Linderman *et al.*, Zero-preserving imputation of single-cell RNA-seq data. *Nat. Commun.* **13**, 192 (2022).
7. A. E. Teschendorff, T. Enver, Single-cell entropy for accurate estimation of differentiation potency from a cell's transcriptome. *Nat Commun* **8**, 15599 (2017).
8. S. Aibar *et al.*, SCENIC: single-cell regulatory network inference and clustering. *Nat Methods* **14**, 1083-1086 (2017).
9. S. Jin *et al.*, Inference and analysis of cell-cell communication using CellChat. *Nat Commun* **12**, 1088 (2021).